

Multiphase Coacervation of Polyelectrolytes Driven by Asymmetry of Charged Sequence

Xu Chen, Er-Qiang Chen,* and Shuang Yang*



Cite This: *Macromolecules* 2023, 56, 3–14



Read Online

ACCESS |



Metrics & More

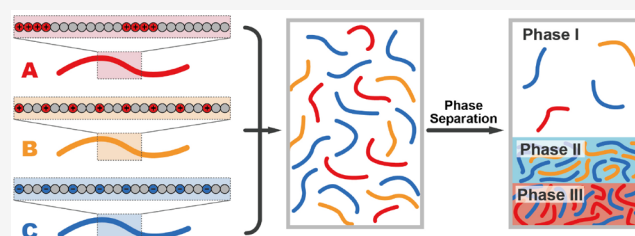


Article Recommendations



Supporting Information

ABSTRACT: The complex coacervation of oppositely charged polyelectrolytes is an important issue, which is relevant to many biological and industrial applications. While various biomolecules have been observed to form hierarchical multiphase structures in cells, its mechanism is still not fully understood. Here, we theoretically study the complex coacervation between the polyanion C and polycations A and B in solution and focus on the influence of charge sequence along the polyions on the multiphase coacervation. The electrostatic free energy is calculated with random phase approximation, and the phase diagrams are constructed by using the convex hull algorithm. It is revealed that the large asymmetry of charge patterns between A and B chains may induce the multiphase separation, driving the formation of two condensed phases, AC coacervate and BC coacervate, coexisting with a dilute phase. On the basis of our result, we propose a good criterion to determine if multiphase separation occurs or not. Furthermore, we analyze the effect of charge sequence of polyanion C as well as the addition of salt on the multiphase coacervation. This work provides insights into the underlying physics of sequence-dependent electrostatic interactions and the design of complex coacervates of polyelectrolyte mixtures.



INTRODUCTION

Liquid biomolecular condensates formed by liquid–liquid phase separation (LLPS) play key roles in cellular processes. The LLPS is essential in functionally compartmentalizing the internal space of cells, providing distinct microenvironments for various biochemical processes.^{1–4} Thus, it is closely related to the formation of membraneless organelles^{5–8} or some human pathologies.^{9,10} In the cellular environment, the LLPS is usually observed for molecules including the intrinsically disordered protein (IDP), exemplified by the well-known nuage protein Ddx4,¹¹ *Caenorhabditis elegans* protein LAF-1,¹² and RNA-binding protein FUS.¹³ These IDPs lack specific ordered three-dimensional structures¹⁴ and are usually rich in polar and charged residues rather than bulky hydrophobic groups,^{15,16} which highlights the importance of electrostatic interaction¹⁷ that may play a major role in driving LLPS.^{18–20} This associative phase separation of oppositely charged polyelectrolytes, named coacervation, can be observed in the solution of polycation and polyanion mixtures^{21,22} or the solution of polyampholytes.^{23,24} Through coacervation, the phase separation into a coacervate phase enriching polyelectrolytes and a coexisted dilute phase with very few polymers will happen.

Many factors affecting the electrostatic interaction could significantly regulate the coacervate process, such as addition of salt ions,^{21,25,26} varying the temperature or dielectric constant of solvents,^{27–30} and tuning the stiffness^{31–34} or structure of charge of polyelectrolytes.^{34,35} Among these factors, the sequence of charge along the polyelectrolyte

chain plays a key role in their LLPS.³⁶ For example, shuffling the sequence of charged residues of wild IDP will regulate their phase separation behavior.^{11,37,38} A key feature of IDPs is the sequence of charged residues, namely, their charge pattern. When the positively and negatively charged residues are arranged into clustered blocks rather than alternating distribution, the mixtures show a higher tendency to form LLPS.¹¹ Similarly, the complex coacervation tendency of the synthesized block copolycation and polyanion will increase when the positive charges are distributed more concentratively, reflected by the higher critical salt concentration (CSC), at which point the condensed phase will dissolve.³⁹ Because of lacking certain folded structures, the IDPs adopt highly dynamic conformations, which breaks the structure–function paradigm of the protein. These different liquid-like structures of IDPs in solution highlight the significance of sequence of residues in determining their phase behavior, in which long-range electrostatic interaction is essential.

Usual LLPS deals with two components of polymer mixtures (irrespective of water solvents). However, a real cellular chemical environment is not a simple two-component solution

Received: June 10, 2022

Revised: October 16, 2022

Published: December 20, 2022



but involves various biomolecules. A variety of molecules are capable of causing LLPS and resulting in multiphase coacervates together with a dilute phase,^{40–42} forming a hierarchical structure such as nucleolus.^{41,43} This multiphase separation can also be generated *in vitro* by a solution containing two different kinds of polycation and one polyanion.^{44–46} The formation of this multiphase structure relies on the type of polyelectrolytes. Some systems will form distinct coacervate phases at equilibrium, while others will only generate a mixture of condensed phases, which difference may originate from the hydrophobic interaction or electrostatic interaction. On the other hand, the variety of coacervate phases is of great significance since various phases can enrich specific small molecules⁴⁴ and thus provide suitable circumstances for corresponding biochemical reactions.⁴⁷ This highlights the significance of understanding the formation of intracellular multiphase structure.

Many theoretical models have been developed to describe the complex coacervation process for weakly charged polyelectrolytes of a two-component system, including the original Voorn–Overbeek (VO) model based on the Debye–Hückel attraction of simple electrolyte⁴⁸ and other refined theories.^{49–61} These theories captured the electrostatic attraction due to collective fluctuation. The VO theory totally ignores the chain connectivity and thus fails to describe the effect of charge sequences. Considering the chain connectivity and intramolecular correlation, the random phase approximation (RPA) method has been developed.^{50–53,62,63} Assuming the ideal Gaussian configuration of polyelectrolytes, the RPA is applicable to dense solution of weakly charged polyelectrolytes.⁵⁴ With the chain connectivity, the RPA framework could capture the effect of monomer sequence,⁶⁴ including the pattern of charged and neutral monomers in the coacervation of oppositely charged polyelectrolytes⁶⁵ or the pattern of positively and negatively charged monomers in the coacervation of polyampholytes.^{66–70} In the dilute branch of phase separation, the chain configuration of polyelectrolyte couples with the charge pattern,⁷¹ and the precise calculation of concentration needs more advanced theories such as field theoretic simulation.^{23,72,73} Besides, for highly charged polyelectrolytes with strong electrostatic interaction, when the driving force of complex coacervation comes from the translational entropy of releasing counterions after complexation between oppositely charged polymers,^{39,74,75} the transfer matrix theory succeeded to describe the coacervation process theoretically and further included the effect of charge pattern.^{76–78} All these theories have found that when the copolyelectrolytes are ranging from alternating to “blocky”, the tendency of coacervation will enhance either by stronger electrostatic correlation or higher translational entropy of free counterions, consistent with the experimental results.

In contrast, there is only limited theoretical work to investigate the multiphase LLPS process of a multicomponent system. For these systems, the key issues include two aspects. The first one is when will the multiphase separation occur and what is the physical mechanism for the appearance of multiphases? The second one is how do the multiphase coacervates vary with the systematic parameters? The driving force of multiphase separation for a multicomponent solution is mostly considered to be the short-range Flory–Huggins interactions.⁷⁹ Then the phase separation can be classified into “demixing”, which means different solutes separate into two individual solutions, and “condensation”, which means solutes

condense into one phase and leaving a dilute phase.^{80,81} When reaching the thermodynamic stable state, this multicomponent mixture may separate into multiphases in terms of the Gibbs phase rule, and the phase diagrams together with the morphology have been studied in detail.^{82,83} However, these discussions are confined to multiphase separation arising from the short-range interaction. Little work has paid attention to the electrostatic force driven multiphase coacervation, especially the effect of charge patterns remains unclear. One related work is to study a two-component polyampholyte solution to modeling two kinds of IDPs; the authors found that with increasing the difference between their charge patterns, the way of two-phase separation will vary from condensation type into demixing type, but the three-phase separation is not observed.⁶⁸

As mentioned before, multiphase coacervation provides a powerful model in understanding subcellular organization (such as membraneless organelles). However, this phenomenon is very complicated as many biomolecules (also means many components and variable parameters) are involved. In order to better understand these complicated systems, we start with a simple but representative modeling system, which contains two kinds of polycations and one polyanion (certainly a system containing two kinds of polyanions and one polycation obeys the same rule), as used by some experiments.^{44–46} Our previous work has already studied this three-component system in which all polyelectrolyte chains are uniformly charged.⁸⁴ The further calculation has shown that if the linear charge densities of two polycations are sufficiently different, the multiple phases will form. Our prediction is consistent with experimental results.^{45,46} In this study, we adopt a similar three-component system but with different charge patterns of polyions to focus on the influence of charge sequence of polyelectrolytes. Concretely, the monomers of polycations A and B (polyanion C) are either positively (negatively) charged or neutral, and their charge sequences are set to be different. The further calculations will predict the detailed phase behavior of this system. Furthermore, we put forward the mechanism that the asymmetry of charge patterns of two polycations also may bring the effective repulsion between different polyelectrolytes, leading to the formation of two coacervates coexisting with a dilute phase. An deep understanding about this representative system may lay a strong foundation for multiphase coacervation. The strategy we used and the underlying mechanism can be extended to systems including more components.

In the following sections, we will give a systematic theoretical study of the influence of charge sequence on multiphase coacervation for the three-component system. First, the RPA method is adopted to calculate the free energy of the mixtures in solution, and then the phase diagrams are constructed by use of convex hull algorithm combined with equal-chemical-potential equations. Then we study how charge sequence asymmetry of A and B could drive a multiphase coacervation process for both periodic and arbitrary charge patterns and put forward a criterion to determine the occurrence of separation between two coacervate phases. The effect of charge sequence of the polyanion is also studied. Finally, we study the effect of salt on this multiphase coacervation and analyze the screening of salt ions.

THEORY AND METHOD

Free Energy Based on Random Phase Approximation.

We consider a homogeneous aqueous solution containing two types of weakly charged polycations (denoted by A and B) and one type of polyanion (denoted by C). All polyelectrolytes have the same Kuhn length $l = 0.85$ nm, which is also set as length unit, consistent with a hydrated monomeric unit length.²¹ The polymerization (or chain length) of these polyelectrolytes is set to be $N_A = N_B = N_C$ unless specified otherwise. The system includes three kinds of different monomers in terms of the charge property. These monomers carry charge of e , 0 , and $-e$ (e is the elementary charge) and are denoted by a , b , and c , respectively. Polycations A and B both consist of positively charged monomer a and neutral monomer b , while polyanion C consists of monomer b and negatively charged monomer c . The fraction of charged monomers is set to be f_I ($I = A, B$, and C). In order to study the influence of charge sequence, polycations A and B have the same fraction of charged monomers ($f_A = f_B$) but different sequences. For simplicity, we assume that the total positive charges of all polycations compensate for the negative charges of polyanions completely. The solution may also include some counterions released from the polyions and added salt ions. We do not distinguish them and see them as salt ions because we treat counterions as a part of the salt. These monovalent small ions carrying charge of $\pm e$ are denoted as s . The solvent is denoted as S . The volumes of monomers, solvents, and small (salt) ions are all assumed to be equal to unit volume l^3 . The number density of each molecule i is ρ_i and its volume fraction is $\phi_i = \rho_i l^3$.

All the polyelectrolyte chains are assumed to adopt the ideal Gaussian chain conformation. We consider weakly charged flexible chains and set the fraction of charged monomers to be low, and the Flory–Huggins parameters between polymers and solvent are set to be 0.5 , so that the polyelectrolyte satisfies Gaussian chain statistics and the counterion condensation effect can be ignored. In order to obtain the free energy of polyelectrolyte solution, we adopt RPA theory taking into account the charge connectivity on polymer chain to capture the electrostatic correlation of charged species. The RPA only considers the Gaussian fluctuation of electrostatic interaction. As the correlation function is in good agreement with Gaussian chain for dense solution of weakly charged polyelectrolytes,⁵⁴ RPA theory with ideal chain conformation can quantitatively fit with simulation results in the coacervate phase.^{23,72,73} Although the RPA theory may break down in the dilute phase,⁷² where the oppositely charged monomers tend to bind together, it is still widely used in the research of coacervation because we are usually concerned more about the dense coacervate phase. Previous papers have well documented the derivation of RPA theory for polyelectrolyte solution^{62,85,86} or polyelectrolyte block copolymer solution.^{66,67} On the basis of these works, the free energy density f of a homogeneous phase can be written as

$$f \equiv \frac{F}{Vk_B T} = f_{F-H} + f_{RPA} \quad (1)$$

where F is the free energy, V the system volume, and k_B the Boltzmann constant. T is the absolute temperature and set to 300 K in this paper. The first term in eq 1 represents the mean-field contribution of corresponding neutral solution and has the form of the Flory–Huggins term

$$f_{F-H} = \sum_i \frac{\phi_i}{N_i} \ln \phi_i + \frac{1}{2} \sum_{ij} \phi_i \phi_j \chi_{ij} \quad (2)$$

where the summations run over all molecules (A, B, C, S, s). It is noted that the salt concentration is defined as $\phi_s = \phi_{s^+} = \phi_{s^-}$. The second term in eq 1 is the electrostatic contribution due to correlations of charge fluctuations, which has the form in RPA framework as

$$f_{RPA} = \frac{l^3}{2} \int \frac{d\mathbf{q}}{(2\pi)^3} [\ln(\det(\mathbf{I} + \mathbf{G}(\mathbf{q})\mathbf{U}(\mathbf{q}))) - \sum_m \rho_m \sigma_m^2 u(\mathbf{q})] \quad (3)$$

where the summation m runs over all type of monomers or small molecules (a, b, c, S, s) and σ_m is the charge carrying by species m . $u(\mathbf{q}) = 4\pi l_B / q^2$ represents the Coulomb interaction between two elementary charges. The Bjerrum length is $l_B = e^2 / (\epsilon_0 \epsilon_r k_B T)$. ϵ_0 is the vacuum permittivity, and $\epsilon_r = 78$ is the relative dielectric constant for water solution. $\mathbf{G}(\mathbf{q})$ is the bare correlation matrix. For our system, it reads

$$\mathbf{G}(\mathbf{q}) = \begin{pmatrix} \rho_A G_A^{aa} + \rho_B G_B^{aa} & \rho_A G_A^{ab} + \rho_B G_B^{ab} & 0 & 0 \\ \rho_A G_A^{ab} + \rho_B G_B^{ab} & \rho_A G_A^{bb} + \rho_B G_B^{bb} + \rho_C G_C^{bb} & \rho_C G_C^{bc} & 0 \\ 0 & \rho_C G_C^{bc} & \rho_C G_C^{cc} & 0 \\ 0 & 0 & 0 & \hat{\rho}_s \end{pmatrix} \quad (4)$$

where $\hat{\rho}_s = \text{diag}(\rho_{s^+}, \rho_{s^-})$ is a 2×2 diagonal matrix for positively and negatively charged salt ions. ρ_I are monomer densities of each type of polyion I . $G_I^{\alpha\beta}$ is the structural correlation function for the polyelectrolyte I and can be calculated as

$$G_I^{\alpha\beta} = \sum_{s_\alpha}^{N_\alpha} \sum_{s_\beta}^{N_\beta} \exp\left(-\frac{q^2 l^2 |s_\alpha - s_\beta|}{6}\right) \quad (5)$$

where s_α and s_β go through all the monomers α and β , respectively, and N_α and N_β are the total numbers of monomer α or β in the polyelectrolyte I . It is noted that the structure factor of solvent in $\mathbf{G}(\mathbf{q})$ is not included since neutral solvents will not contribute to the electrostatic correlations. $\mathbf{U}(\mathbf{q})$ is the electrostatic interaction matrix, and its elements can be written as $U_{ij}(\mathbf{q}) = \sigma_i \sigma_j u(\mathbf{q})$. The last term in eq 3 is the self-energy of salt ions, which need to be subtracted to guarantee the convergence of the integral at large q .

Construction of Phase Diagram. With the free energy density of polyelectrolyte solution, the phase diagram can be constructed and the condition of multiphase coacervation may be found. In the absence of salts and counterions, the free energy density can be expressed as $f_{\text{tot}} = f(\phi_A, \phi_B)$ because the concentration of polyion C is determined in terms of the electroneutrality condition. Phase separation will occur if the two or three coexisting new phases have a lower total free energy than that of homogeneous bulk phase. The minimization of f_{tot} is equivalent to finding the lower convex hull of the free energy surface, the method of which developed by Qhull⁸⁷ is adopted in our study. With the composition space divided into small grids, the free energy of each grid point together with their convex hull surface can be calculated. The points where convex hull is consistent with free energy surface are stable monophasic regions, and for the other points where convex hull shows a lower f_{tot} than original surface, this lower total free energy can be reached by phase separation into two or three coexisting phases, depending on the shape of

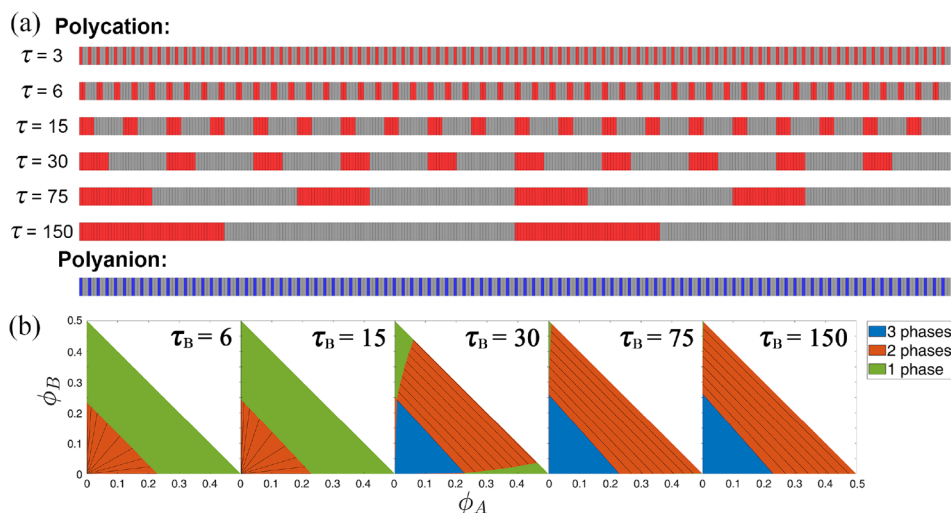


Figure 1. (a) Charge pattern of polyelectrolytes in our system. The total chain length is $N = 300$, and the length of repeating unit is defined as τ . Red, blue, and gray squares denote positively charged, negatively charged, and neutral monomers, respectively. (b) Phase diagram of salt-free solution of polycations A and B and polyanion C. A and B have the same charge fraction but different charge patterns. $\tau_A = \tau_C = 3$ and $\tau_B = 6, 15, 30, 75$, and 150 . $\phi_C = (\phi_A + f_A + \phi_B + f_B)/f_C$. The Flory–Huggins parameters between polymers and solvent are set as 0.5. Blue, red, and green denote 3-phase, 2-phase, and 1-phase region, respectively. Black lines of the 2-phase region are tie-lines of phase separation.

convex hull surface. The details of this method can be referred to in some previous papers.^{82,84,88}

When salt is added, the system becomes more complicated. The increase in the dimensions of composition space makes it harder to compute a high-dimensional convex hull. Therefore, the formulas expressing chemical potential equilibrium need to be solved to get the phase diagram. At equilibrium, one has equal chemical potentials as $\mu_{i,I} = \mu_{i,II} = \mu_{i,III}$ among different phases, where μ denotes the chemical potential, i denotes all independent species including A, B, salt, and water in our system, and I, II, and III represent different phases. By using the obtained concentrations at equilibrium for a salt-free system as the initial values, one can gradually increase the salt concentration and solve the formulas to determine the concentrations of each phase, until each species has the same chemical potential in all phases.

RESULTS AND DISCUSSION

Phase Diagram of Periodic Charge Sequence. We first investigate the phase diagram of three-component salt-free solution containing polyelectrolytes A, B, and C. All polyelectrolytes have the same chain length of $N_A = N_B = N_C = N = 300$ and the fraction of charged monomers of $f_A = f_B = f_C = 1/3$, which is weakly charged and suitable for RPA theory. The Flory–Huggins parameters χ between polymers and solvent are set as 0.5 so that the solvent will be athermal solvent for polymers, and the remaining χ are all 0. These parameters are fixed unless specified otherwise. In this section, the polyelectrolytes are set to have periodic charge patterns. Different sequence polyions have the same total number of charges, and each sequence polyelectrolyte chain is composed of several repeating sections or blocks (each block consists of charged monomers followed by neutral monomers). Therefore, we specify the sequence of polyions by a parameter τ that is the length of repeating block, in which $\tau/3$ charged monomers are followed by $2\tau/3$ neutral monomers. For example, $\tau = 15$ indicates that each block includes 5 charged monomers and 10 neutral monomers, and each polymer consists of 20 same blocks. A small τ value denotes a more

dispersed distribution of charges along the chain. In this part, we set τ to be 3, 6, 15, 30, 75, and 150 for polycations A and B. For the polyelectrolytes with very long block length, they will likely undergo microphase separation and form micelles,⁸⁹ especially for diblock copolymers.⁷⁸ In the present work, we will focus on the polyelectrolytes being only capable of undergoing macrophase separation, which leads to the LLPS. The corresponding charge pattern is shown in Figure 1a. The charge sequence effect of the polyanion on the multiphase separation will be further discussed in the next section.

For the system with similar charge sequences of A and B components, multiphase coacervation should not be observed. Furthermore, our calculations show that three-phase separation is possible once τ_A and τ_B are different enough. Figure 1b displays the phase diagrams of the solution consists of polycations A and B and polyanion C with $\tau_A = 3$ and $\tau_B = 6, 15, 30, 75$, and 150 . Other similar phase diagrams of $\tau_A = 6, 15, 30$, and 75 are shown in the Supporting Information. The x - and y -axes of the phase diagram denote the volume fraction of polycations A and B, respectively; the concentration of the polyanion C is calculated by use of electroneutrality condition through $\phi_C = (\phi_A + f_A + \phi_B + f_B)/f_C$, and the volume fraction of water is derived from the incompressibility as $2\phi_S = 1 - \phi_A - \phi_B - \phi_C$. The green region on the phase diagram denotes the single-phase region, where the macrophase separation will not happen. The red region denotes the coexisting two-phase region. When the bulk concentration of solution is within this region, it will phase-separate into two phases, and the composition of them is denoted by the black tie lines. The blue region denotes the three-phase region, where the solution undergoes multiphase separation into a dilute phase, an AC-rich coacervate phase, and a BC-rich coacervate phase, denoted by phases I, II, and III, respectively.

For the cases of $\tau_A = 3$ and $\tau_B = 6$ and 15, the multiphase separation will not happen since B has a similar charge pattern to A. When the bulk concentration is low, the solution will separate into a dilute phase together with a coacervate phase consisting of A, B, and C polymers, indicated by the tie-lines.

When τ_B is larger than 30, the 3-phase separation will happen at the low bulk concentration, demonstrating three coexisting phases (I, II, and III) shown by the three vertexes of the blue triangle. Meanwhile, the 2-phase separation into the AC and BC solution phases will happen at the higher bulk concentration. This multiphase separation for the systems with large difference between τ_A and τ_B can further be observed in the phase diagrams of the Supporting Information, where τ_A has more values. This indicates that the asymmetry of charge sequence may drive a multiphase separation.

The above calculations indicate that the difference in the charge distribution pattern along two polycations may bring additional immiscibility between them, which is the same as the immiscibility induced by the asymmetry of linear charge density in our previous study.⁸⁴ Likewise, the effective repulsion arising from the electrostatic correlation can be defined. The second-order variation of electrostatic free energy can be written as

$$\delta^2 f_{\text{RPA}} = - \sum_{ij} \frac{1}{2} \int \frac{d\mathbf{q}}{(2\pi)^3} \left[\frac{a(\mathbf{q})G_i(\mathbf{q})G_j(\mathbf{q})}{N_i N_j} \right] \delta\phi_i \delta\phi_j \quad (6)$$

where G_i denotes G_A^{aa} , G_B^{aa} , or G_C^{cc} for polyelectrolytes, and $G = 1$ for salt. $a(\mathbf{q})$ is a prefactor and has the form

$$a(\mathbf{q}) \equiv \frac{u(\mathbf{q})^2 l^3}{(l^3 + \sum_m \phi_m G_m(\mathbf{q}) u(\mathbf{q}) / N_m)^2} \quad (7)$$

The above summation in the denominator runs over all charged species m and is independent of specific ij . In terms of eq 6, one can define an effective Flory–Huggins parameter χ_{eff} between any pair of components as

$$\chi_{\text{eff},ij} = \chi_{ij} - \int \frac{d\mathbf{q}}{(2\pi)^3} [a(\mathbf{q})G_i(\mathbf{q})G_j(\mathbf{q})/N_i N_j] \quad (8)$$

Furthermore, by use of the incompressibility constraint $\sum_i \delta\phi_i = 0$, the $\chi_{\text{eff},ij}$ can further be modified to $\chi'_{\text{eff},ij}$ so that the diagonal elements satisfy $\chi'_{\text{eff},ii} = 0$ while keeping $\delta^2 f$ unchanged. This new $\chi'_{\text{eff},ij}$ takes the form

$$\chi'_{\text{eff},ij} = \chi_{ij} + \frac{1}{2} \int \frac{d\mathbf{q}}{(2\pi)^3} [a(\mathbf{q})(G_i(\mathbf{q})/N_i - G_j(\mathbf{q})/N_j)^2] \quad (9)$$

It is noted that in the expression $\chi'_{\text{eff},ij}$, i and j refer to the type of molecule A, B, or C rather than the monomer species a, b, or c. It means that in the definition of $\chi'_{\text{eff},ij}$, the polyelectrolytes are considered as integral molecules instead of copolymers with different patterns. This equation indicates that the difference in charge pattern will lead to an effective repulsion between polyelectrolytes. When there is repulsion between polycation and polyanion, they will still keep in one phase to fulfill electroneutrality. On the other hand, although the polycations A and B have the same chain length and composition, the asymmetry in their charge pattern may bring an effective repulsion between them and lead to the separation between two coacervate phases.

With the above prediction, one expect to observe that same charged polyelectrolytes with different charge patterns may condense in different coacervate phases in experiments or simulations. Unfortunately, there lacks such works currently to investigate how charge patterns affect multiphase coacervation. We also note that in the study by Boeynaems et al. mixing a positively charged polymer (PR) with two different negatively

charged homopolymeric RNAs (poly rA and poly rC) in water generates two coexisted condensates.⁹⁰ Using coarse-grained simulations, the authors confirmed that multiple phases could be achieved since poly rA preferentially bind PR over poly rC, and the specific short-range interactions provided driving force in the formation of multiple condensates via complex coacervation. The above calculation for our system indicates the large asymmetry of charge patterns of polyions may generate different attractions to oppositely charged polymers (accordingly producing effective repulsion between same charged polyions), which gives the similar mechanism as Boeynaems et al.'s work. On the other hand, the prediction on our previous article about the multiphase coacervation driven by asymmetry of linear charge density⁸⁴ is in accord with experiments.^{45,46} Specifically, a recent work by Donau et al. shows a mixture of two miscible polyanions in water will form multiphase droplets with adding positively charged peptide,⁹¹ in which the asymmetry of linear charge density should play an important role, demonstrating the robustness of our calculation. Therefore, we believe the charge patterns is important in regulating multiphase coacervation and hope our theoretical predictions can receive further direct evidence from experiments or simulations.

In eq 9 the $\chi'_{\text{eff},ij}$ involves a complicated integration, and it is not easy to directly relate the immiscibility to the difference of charge sequence; thus, a more convenient criterion should be established. As confirmed by other researchers, for a simple solution consisting of binary oppositely charged polyions, the concentration of coacervate phases depends on the charge sequence of polycation if polyanions are the same. Compared to the case of polycations with alternating charge sequence, the polyelectrolytes with blocky charge pattern exhibit higher concentration of polyions in the coacervate phase and higher critical salt concentration,³⁹ indicating a higher tendency of coacervation. The coacervation tendency depends on the electrostatic correlations. Effectively, the polyanions attract the polycations with longer block lengths more strongly, and the coacervation tendency is stronger, resulting in higher polymer concentration in the coacervate phase. When two polycations have rather different charge patterns, the attractions from polyanions may be different enough so that the two polycations are effectively repelling, and 3-phase coexistence may occur. Therefore, we suggest a method to judge whether 3-phase separation occurs or not for the ABC tricomponent system, based on the coacervate phase property of 2-phase separation for the binary system containing one type of polycations and one type of polyanion. Considering an A + C polyions solution, we denote the polycation concentration in the coacervate phase as ϕ_p^A . Similarly, we denote the polycation concentration in the coacervate phase as ϕ_p^B for a B + C binary polyion solution. Then the composition difference $\Delta\phi_p = |\phi_p^A - \phi_p^B|$ may represent qualitatively the difference of coacervation tendency with polyanions for two kinds of polycations, and we choose it as the criterion of 3-phase coexistence. When $\Delta\phi_p$ is large enough, the polyanions have a stronger preferred attraction to one polycation (for example, A) than the other polycation (B). In this case, if A, B, and C polyions are mixed together, multiphase separation may occur, and a dilute phase coexisting with two coacervate phases (AC and BC) is possible.

To quantify this point, we consider a binary mixture solution containing oppositely charged polyions. The polyanion has a

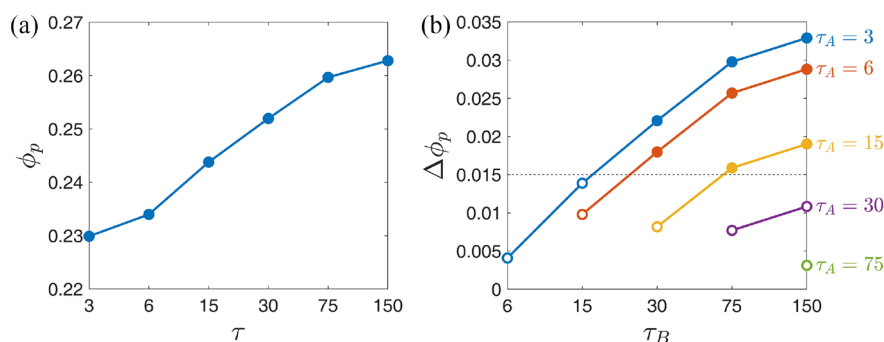


Figure 2. (a) Concentration of polycation in the coacervate phase varies with their charge pattern for two-component mixture consisting of a type of polycations with varying τ and a type of polyanion with fixed $\tau = 3$. (b) For a three-component solution containing A, B, and C polyions, $\Delta\phi_p$ is calculated by considering two separate systems (A + C and B + C solutions) with given τ_A and τ_B values. At the same time, whether these three-component systems can undergo 3-phase separation is displayed accordingly. The solid circles denote the solution may separate into a dilute phase coexisted with two coacervate phases, while hollow circles denote it can only separate into a dilute and a coacervate phase.

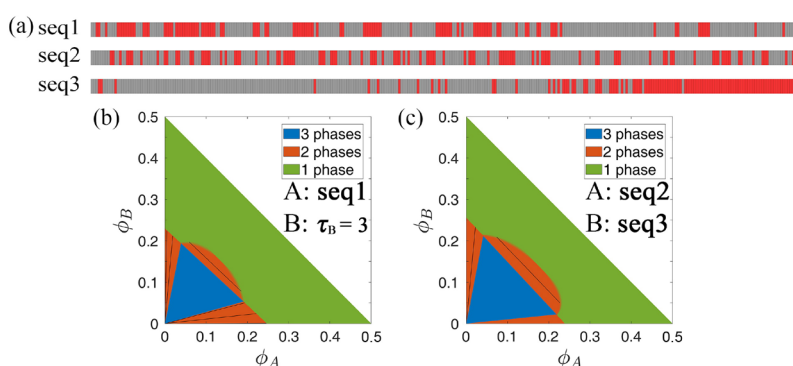


Figure 3. (a) Some arbitrary charge sequences of polycations. Red and gray squares denote positively charged and neutral monomers, respectively. (b, c) Phase diagram of salt-free solution of polycation A, B, and polyanion C mixture solution. A and B have the same fraction of charged monomers but different charge patterns. Polyanions C has periodic charge sequence of $\tau = 3$. In (b), polycation A has the sequence 1 and polycation B has periodic charge sequence of $\tau = 3$. In (c), polycation A has the sequence 2 and polycation B has sequence 3. Blue, red, and green denote the 3-phase, 2-phase, and 1-phase region, respectively. Black lines of the 2-phase region are tie-lines of phase separation.

fixed value of $\tau = 3$, while the τ value of polycation varies from 3 to 150. By setting the bulk concentration of the other polycations as zero, we calculate the concentration of polycation in coacervate phase and plot it in Figure 2a. One can see that the coacervate phase has higher concentration of polycations for larger τ . Our target is a three-component system consisting of two types of polycations (A and B) and one type of polyanion (C). Therefore, we consider two individual two-component systems, namely, A + C and B + C mixtures. Figure 2b displays the $\Delta\phi_p$ for different combinations of τ_A and τ_B . Here we only need to consider when $\tau_B \leq \tau_A$. At the same time, we also give the information for three-component solution with a given τ_A for polycation A and τ_B for polycation B in Figure 2b. The solid circles denote that the multiphase separation may happen for the system with given τ_A and τ_B , and the solution will separate into a dilute phase which coexisted with two coacervate phases of AC and BC in some region of the phase diagram. The hollow circles denote it will only separate into a dilute phase and an A + B + C coacervate phase, and three-phase separation is absent. An important finding is that when $\Delta\phi_p$ is larger than some value $\Delta\phi_p^*$, all three-component systems exhibit three-phase separation. Meanwhile, the system with $\Delta\phi_p \leq \Delta\phi_p^*$ only exhibits a 2-phase separation. Therefore, $\Delta\phi_p^*$ provides a good criterion to determine the appearance of multiphase separation. The critical $\Delta\phi_p^*$ for a multiphase separation should be related to

many factors including the chain length, charge fraction, strength of electrostatic interaction, etc. In our system, we can find that $\Delta\phi_p^*$ is around 0.015.

Phase Diagram for Polycations with Arbitrary Charge Sequences. The charge patterns of polycations are extended to arbitrary charge sequence in this part. We have generated a series of polycations with arbitrary charge distribution along the chain, keeping the chain length and fraction of charged monomers to be constants as $N = 300$ and $f = 1/3$. We have selected three types of polycations with typical sequences as shown in Figure 3a. For each charge sequence, we also calculate the polycation concentration ϕ_p in coacervate phase when the corresponding polycations complex with periodically charged polyanion with $\tau = 3$. These concentrations are $\phi_p = 0.247$, 0.239, and 0.256 for sequence 1, 2, and 3, respectively. Then we calculate the phase diagram of three-component solution in which the polycations may have arbitrary charge sequences. The polyanion C has periodic sequence of $\tau = 3$. When polycation A has an arbitrary sequence 1 and B has a periodic sequence of $\tau = 3$, a typical phase diagram is shown in Figure 3b. Also, for a system in which A has sequence 2 and B has sequence 3, a typical phase diagram is shown in Figure 3c. Both two diagrams have a blue 3-phase region, indicating that for arbitrary sequences the asymmetry in sequence can also produce an effective repulsion between polycations and may lead to multiphase separation. When we use the convex hull

method to draw phase diagram, the calculation error relies on how small the grids are in dividing the phase space. Therefore, the position of the critical point in the diagonal 2-phase region cannot be determined precisely. Instead, the critical point should lie on the right upper phase boundary of 1- and 2-phase region. Considering the sequence 1 and 3 statistically having blocky charge patterns, the separation of these polycations with nearly alternating distributed charge sequences is reasonable. On the other hand, phase diagrams b and c reveal that ϕ_B in phase II (AC-rich coacervate) and ϕ_A in phase III (BC-rich coacervate) are non-negligible, indicating the immiscibility between two coacervate phases is weak. We further find that for systems in Figure 3b,c $\Delta\phi_p = 0.017$, which is a little larger than the critical value $\Delta\phi_p^* = 0.015$ we founded in the previous section.

Likewise, more arbitrary sequences with fraction of charged monomers of $f = 1/3$ are generated for polycations. For each arbitrary sequence, we first calculate the concentration of polycations ϕ_p in the coacervate phase when the polycations are simply mixed with polyanion of periodic sequence $\tau = 3$. Then the phase diagrams of the solution containing two types of polycations with different arbitrary sequences and polyanions of $\tau = 3$ are calculated. These phase diagrams are classified into two categories: one that 3-phase separation may happen and another one that would only undergo 2-phase separation. For each system with given arbitrary charge sequences for A and B polycations, $\Delta\phi_p$ is also calculated. We handle 1500 systems with different combinations of charge sequences for A and B polymers from 3000 sequences generated arbitrarily. After calculating their $\Delta\phi_p$ and phase behaviors, we give the results as shown in Figure 4. The solid circles represent the systems that can phase-separate into three coexisting phases, while the hollow circles mean only 2-phase separation happens and multiphase coacervation cannot occur.

Apparently, it can be observed in Figure 4 that $\Delta\phi_p^* = 0.0155$ can approximately be a criterion for the appearance of multiphase separation. When the $\Delta\phi_p$ is above $\Delta\phi_p^*$, the

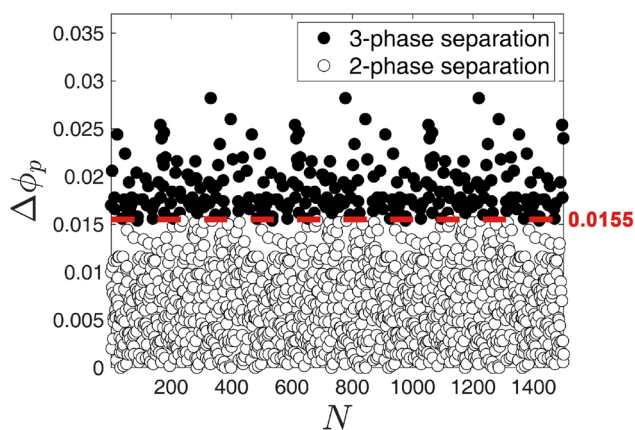


Figure 4. Phase behavior of different systems consisting of two kinds of polycations with arbitrary sequences and polyanion with periodic sequence of $\tau = 3$. N denotes different systems we arbitrarily generated, and the $\Delta\phi_p$ denotes the differences of ϕ_p , which is the concentration of the polycation in the coacervate phase when they individually coacervate with the $\tau = 3$ polycation. The solid circles denote the systems may undergo a 3-phase separation, while the hollow circles denote there will only be 2-phase separation. The red line of $\Delta\phi_p = 0.0155$ can be approximately seen as a criterion of multiphase separation.

immiscibility between two polycations is capable of driving the phase separation between two coacervate phases and leading to a 3-phase separation. Figure 4 determines more precisely the critical value as $\Delta\phi_p^* = 0.0155$. Therefore, $\Delta\phi_p$ can quantify the immiscibility of two polycations in three-component solution, whatever their charge patterns. On the other hand, although this criterion is general for all charge patterns of polycations, the specific critical value depends on system details, including the charge fraction and chain length of polycations and the structure of polyanion.

Charge Sequence Effect of Polyanion. In previous sections, the charge pattern of polyanion is fixed and the charge sequence effect of polycation is investigated. In this section, we study the charge sequence effect of polyanion on the multiphase separation. The structure of polycations are fixed, where polycations A and B have the chain length of $N_A = N_B = 120$, the fraction of charged monomer of $f_A = f_B = 1/3$, and periodic sequence of $\tau_A = 3$ and $\tau_B = 60$; i.e., polycation A has the sequence of $(ab_2)_{40}$ and B has $(a_{20}b_{40})_2$. The chain length and charge fraction of the polyanion are fixed at $N_C = 120$ and $f_C = 1/3$, and its charge sequence is set to be periodic patterns with $\tau_C = 3, 15$, and 60.

The phase diagrams of three-component solution consisting of A, B, and C are depicted in Figure 5. It can be seen that with increasing τ_C , the three-phase window (blue region) decreases and the two-phase region (red) of demixing phases shrinks. At the same time, both the concentration of B (ϕ_B) in phase II and concentration of A (ϕ_A) in phase III (corresponding to the two corners of blue triangle) increase. The results indicate that the immiscibility between two coacervate phases decreases when the charge pattern of the polyanion becomes blockier.

Meanwhile, with the increase of τ_C , the total concentration of polyelectrolyte ϕ_p in coacervate phase for two-component AC solution or BC solution increases, indicated by the expansion of the 2-phase region along the coordinate axes of ϕ_A or ϕ_B . This higher coacervation tendency induced by the blockier charge pattern has been well described in the previous works,^{39,65,76} which physically arises from the stronger attraction between negatively charged polyions and positively charged polyions. However, in the three-component solution, this higher concentration of ϕ_p will further produce a lower immiscibility between two coacervate phases. Equation 9 shows that the effective repulsion between two polycations originates from the asymmetry of structure factor $G(\mathbf{q})$ and the constant $a(\mathbf{q})$. When polyanions change their charge pattern and polycations' charge sequences are fixed, the difference in structure factor $G(\mathbf{q})$ between A and B is a constant, and only $a(\mathbf{q})$ is affected. On the other hand, eq 7 shows that $a(\mathbf{q})$ is related to the electrostatic interaction $u(\mathbf{q})$ and the summation of $\phi Gu/N$. Therefore, the latter term plays an effective screening role in electrostatic interaction. Once the concentration of polyelectrolyte ϕ_p is increased, $\chi'_{\text{eff,AB}}$ will become smaller, meaning that the electrostatic interaction will be further screened and thus results in the decrease of immiscibility. In Figure 5, increasing τ_C leads to the increase of ϕ_p in coacervate phase, and consequently the decreased tendency of multiphase separation. As before, many factors, including the charge pattern of polyanion, chain length, and fraction of charged monomers, all have an impact on the multiphase coacervation, and the details can be referred to in the Supporting Information. When the polyanion shows a higher coacervation tendency with polycations, the separation

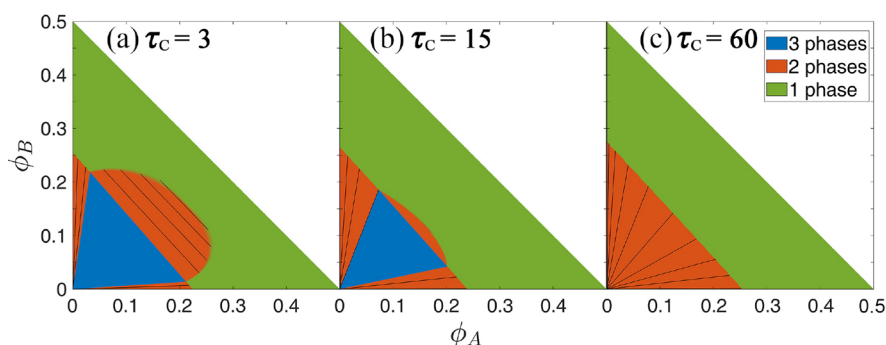


Figure 5. Phase diagram of salt-free solution of polycations A and B and polyanion C. Polymers have chain length of $N_A = N_B = N_C = 120$, fraction of charged monomers of $f_A = f_B = f_C = 1/3$, and periodic sequence of $\tau_A = 3$, $\tau_B = 60$, and $\tau_C =$ (a) 3, (b) 15, and (c) 60. Blue, red, and green denote 3-phase, 2-phase, and 1-phase region, respectively. Black lines of the 2-phase region are tie-lines of phase separation.

between coacervate phases is less possible because of stronger screening.

Phase Diagram with Adding Salt. For a common two-component system, adding salts can screen electrostatic interaction and may lead to the coalescence between the dilute and coacervate phase. Here we investigate the salt effect on multiphase separation of polyions driven by asymmetry in charge sequence. Because the electroneutrality condition has been guaranteed with stoichiometry of oppositely charged polymers, the salt added includes equivalent monovalent cations and anions, and its concentration is denoted by $\phi_s = \phi_s^+ = \phi_s^-$.

We calculate the composition of each phase for 3-phase separated systems when salt is gradually added into the solution, and three-dimensional phase diagrams of two typical systems are shown in Figure 6. The polyelectrolytes are set to

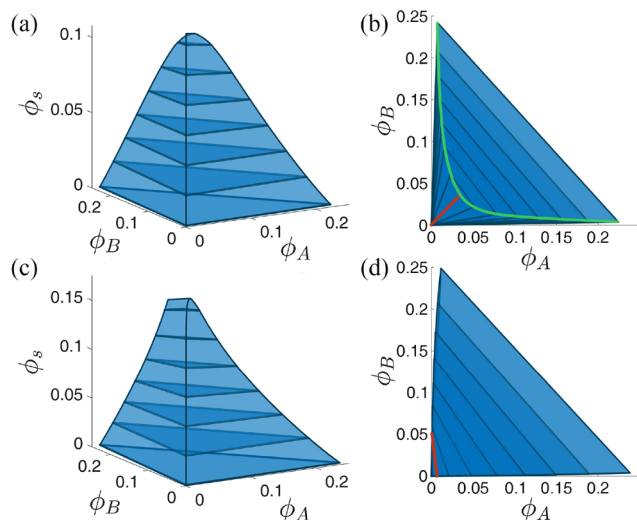


Figure 6. Phase diagrams of solution of polycations A and B and polyanion C when salt is added. The blue region denotes 3-phase separation. The deep blue surfaces denote the tie lines of 3-phase separation. Polyelectrolytes have a chain length of $N_A = N_B = N_C = 300$, charge fraction of $f_A = f_B = f_C = 1/3$, and periodic sequence of $\tau_C = 3$, (a, b) $\tau_A = 3$, $\tau_B = 30$; (c, d) $\tau_A = 15$, $\tau_B = 150$. (b, d) Top views of phase diagram (a, b). The end points of red lines denotes the composition of two phases at the critical salt concentration for 3-phase separation. In (b), when 3-phase separation turns into 2-phase, the region below the green line denotes dilute-ABC separation, and above it denotes AC-BC separation.

have periodic charge patterns. The charge sequence of polyanion is set to be $\tau_C = 3$, while polycations have the parameter as $\tau_A = 3$ and $\tau_B = 30$ in Figure 6a,b and $\tau_A = 15$ and $\tau_B = 150$ in Figure 6c,d. With the addition of salt, the 3-phase region shrinks due to the screening of salt ions. At the critical salt concentration where the coexisting 3-phase disappears, the composition of two phases becomes the same, which indicates that the 3-phase separation transforms into a 2-phase separation. However, these two systems show a different dissolution way with adding salt. For $\tau_A = 3$ and $\tau_B = 30$ in Figure 6a,b, the compositions of two coacervate phases approach gradually and become the same at the critical salt concentration. When the bulk concentration lies in the above region of green line in Figure 6b, addition of salt will lead to the disappearance of the dilute phase, and the left two phases are coexisting AC and BC solutions. If the bulk concentration is below the green line, the two coacervate phases will fuse, forming a condensed A + B + C coacervate phase together with a dilute phase. For the system with $\tau_A = 15$ and $\tau_B = 150$ (Figure 6c,d), the 3-phase region also shrinks with addition of salt, but the compositions of AC coacervate phase and the dilute phase approach rapidly and become the same at the critical point. Therefore, the dilute phase disappears finally, and the solution consists of two coexisting phases: one is condensed AC phase, and another one is the homogeneous B + C solution with low polyelectrolyte concentration. In our previous work about multiphase separation driven by linear charge asymmetry, salt will only induce the coalescence of dilute phase and one coacervate phase containing polycations with lower charge density.⁸⁴

Either the fusion between two coacervate phases or the dissolution of the AC coacervate phase into the dilute phase indicates the screening effect of mobile ions on electrostatic correlation. Considering the attractive interaction between C and A/B chains as well as the repulsive interaction between A and B chains, salt ions should induce the screening effect in a complicated way. To reveal the different roles of salts in the above two systems, we plot the concentration variations of A/B components with added salts for different phases. Figure 7a,c gives the concentrations of polyions A and B within different phases as functions of salt concentration for coexisting three phases. Note that the concentration of C should be equal to the sum of that of A and B in each phase as a result of electroneutrality. It can be seen that adding salts decreases all concentrations of major components in coacervate phases, for example, ϕ_A in phase II (AC coacervate) and ϕ_B in phase III (BC coacervate), which indicates the strong screening role of

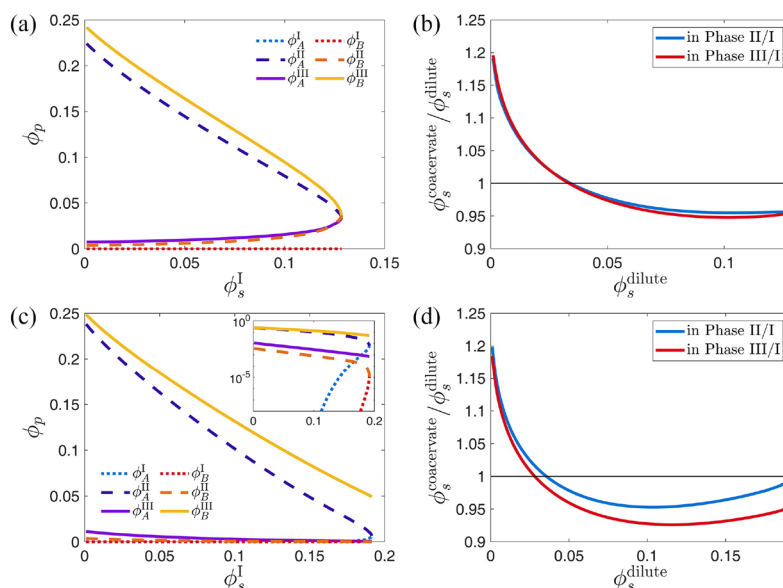


Figure 7. (a, b) When multiphase separation happens, the concentrations of ϕ_B and ϕ_A in phases II and III as functions of salt concentration for the system with (a) $\tau_A = 3$, $\tau_B = 30$ and (b) $\tau_A = 15$, $\tau_B = 150$. The dashed and solid lines denote phase II and III, respectively. The polyanion C is periodic sequence with $\tau_C = 3$. (c, d) Variation of salt partition between coacervate phases (II, III) and dilute phase I with salt concentration for the system with (c) $\tau_A = 3$, $\tau_B = 30$ and (d) $\tau_A = 15$, $\tau_B = 150$.

salt ions between oppositely charged polyions. The electrostatic correlations are weakened significantly.

An interesting phenomenon is that the influence of salts on the minority component in each condensed phase is rather different for the above two systems. For the system with $\tau_A = 3$ and $\tau_B = 30$, the addition of salts increases the content of minor components in each condensed phase gradually, such as ϕ_A in BC coacervate and ϕ_B in AC coacervate, as shown in Figure 7a. In this case, salt ions also screen the repulsive interaction between polycations A and B. However, the system with $\tau_A = 15$ and $\tau_B = 150$ exhibits opposite dependence of minor components' concentrations on the salt concentration. Figure 7c shows that addition of salt ions leads to the decreasing of minor polycation concentrations for two coacervate phases, including ϕ_A in the BC coacervate and ϕ_B in the AC coacervate. At the same time, the AC condensed phase coalesces with the dilute phase at high salt concentration. Therefore, adding salt effectively results in a stronger separation tendency between A and B polycations in this case. This effect is possibly related to the difference in electrostatic correlation $\Delta G(q) = |G_A - G_B|$ between two polycations, although the underlying mechanism remains unclear. The system with large sequence asymmetry of $\tau_A = 15$ and $\tau_B = 150$ displays a significant strong peak while the system with $\tau_A = 3$ and $\tau_B = 30$ only has a weak wave crest at larger q (see Figure S4). For polyelectrolyte mixture, the large asymmetry of sequence pattern between A and B polycations produces stronger repulsive correlations, which may be slightly affected by the screening of salt ions. At last, we study the salt partitioning in the coexisting phases for the above two systems, as shown in Figure 7b,d. At low salt concentrations, the small ions are enriched in both AC and BC coacervates, and the small ion concentrations in condensed phases are higher than that in dilute phase by even about 20%, which is attributed to the stronger electrostatic correlations in coacervates. At high salt concentrations, salts are depleted from two coacervate phases to dilute phase.

CONCLUSIONS

The study theoretically investigates the complex coacervation of solution consisting of polycations A and B and polyanion C, where A and B have the same charge fraction but different charge patterns. The phase diagrams of the solution are calculated by use of RPA for various charge patterns, and the effects of charge sequence of polyanion as well as addition of salt are also studied. The calculations indicate that the charge pattern of polyelectrolytes has a significant influence on regulating the coexisting phases of LLPS. On the basis of our results, some general conclusions can be reached.

First, the large enough asymmetry of charge patterns of polyelectrolytes in a three-component system may lead to an effective repulsion between different same-charged components and consequently result in the occurrence of multiphase separation. In our system, when the sequences of polycations are similar, it will only phase-separate into a dilute phase together with an A + B + C coacervate phase. However, if polycations A and B have distinct charge patterns, multiphase separation happens and a dilute phase will coexist with two coacervate A + C and B + C phases.

Second, we put forward a criterion capable of predicting the occurrence of multiphase separation. The criterion is the difference of polyelectrolyte concentration in coacervate phases, $\Delta\phi_p = \phi_p^A - \phi_p^B$, when the individual coacervation process of two polycations with polyanions (A + C solution or B + C solution) is taken into account. If $\Delta\phi_p$ is larger than some critical value of $\Delta\phi_p^*$, the immiscibility between two coacervate phases becomes large enough, and then the multiphase structure will form no matter periodic or arbitrary charge sequence of polycations. A lot of different phase behaviors for various arbitrary charge sequences, as shown in Figure 4, further confirm the validation of the criterion $\Delta\phi_p$. Specifically, with our chosen systematic parameters, $\Delta\phi_p^* = 0.0155$ approximately in this study.

Third, our results show that the properties of counterpolyion (polyanion), such as its charge sequence, will affect the

multiphase separation. When its charge sequence of polyanion becomes blockier, the immiscibility of two coacervate phases decreases, which originates from the higher concentration of polyelectrolytes in the coacervate phases. The screening of electrostatic interaction is enhanced for more concentrated polyelectrolyte solution, and thus the separation tendency between coacervate phases is weakened. Therefore, the phase separation between coacervate phases will be less likely to occur.

At last, salt ions have a remarkable effect on phase separation since they also enhance the screening of electrostatic correlation interaction. We investigate the variation of 3-phase region with addition of salt ions. Depending on specific system and initial solution compositions, adding salt may result in the dissolution of one coacervate phase into the dilute phase while retaining another coacervate phase or the fusion between two coacervate phases coexisting with a dilute phase.

Although all the results are calculated for a three-component coacervation system, we believe that the mechanism of sequence asymmetry-driven multiphase coacervation, as well as the robust conclusion, can be extended to general LLPS systems including more components. It is need to be point out that the RPA theory we used has its limitations. For the dilute phase, RPA fails to give an accurate description of the free energy as the chains may deviate from Gaussian conformation significantly. Second, RPA is based on the homogeneous concentration assumption, and it may not capture the correct structure for highly blocky polycations (such as diblock polycations) in the coacervate phase. In that case, microphase separated structure may appear, in which dense domains of charged blocks coexist with the regions enriched with neutral blocks, as confirmed by theory⁷⁸ and simulation.⁸⁹ Besides, the charge association and dissociation may play extremely important roles in determining the properties of polyelectrolyte coacervation system, which is not included in the present study. In our model, we only consider weakly charged polyelectrolytes and assume that the charges of each chain remain fixed. The complex charge association and dissociation effect still need further development. Despite these limitations, our work based on RPA theory reveals the importance of charge pattern to drive a multiphase coacervation for multicomponent polyelectrolyte mixture, and it provides some insights into the formation of multiphase structures in cells.

■ ASSOCIATED CONTENT

SI Supporting Information

The Supporting Information is available free of charge at <https://pubs.acs.org/doi/10.1021/acs.macromol.2c01205>.

More phase diagrams of coacervation of polyelectrolytes with periodic sequences, the way to generate the arbitrary charge sequences, the effect of polyanion's chain length and charge fraction, and some further discussion of effect of salt (PDF)

■ AUTHOR INFORMATION

Corresponding Authors

Er-Qiang Chen – Beijing National Laboratory for Molecular Sciences, Key Laboratory of Polymer Chemistry and Physics of Ministry of Education, Center for Soft Matter Science and Engineering, College of Chemistry and Molecular Engineering,

Peking University, Beijing 100871, China; orcid.org/0000-0002-0408-5326; Email: eqchen@pku.edu.cn

Shuang Yang – Beijing National Laboratory for Molecular Sciences, Key Laboratory of Polymer Chemistry and Physics of Ministry of Education, Center for Soft Matter Science and Engineering, College of Chemistry and Molecular Engineering, Peking University, Beijing 100871, China; orcid.org/0000-0002-5573-5632; Email: shuangyang@pku.edu.cn

Author

Xu Chen – Beijing National Laboratory for Molecular Sciences, Key Laboratory of Polymer Chemistry and Physics of Ministry of Education, Center for Soft Matter Science and Engineering, College of Chemistry and Molecular Engineering, Peking University, Beijing 100871, China

Complete contact information is available at:

<https://pubs.acs.org/10.1021/acs.macromol.2c01205>

Notes

The authors declare no competing financial interest.

■ ACKNOWLEDGMENTS

The authors acknowledge financial support from the National Natural Science Foundation of China (NSFC) (Grants 22073002, 21634001, and 21674005).

■ REFERENCES

- (1) Brangwynne, C. P.; Tompa, P.; Pappu, R. V. Polymer physics of intracellular phase transitions. *Nat. Phys.* **2015**, *11*, 899–904.
- (2) Bergeron-Sandoval, L.-P.; Safaee, N.; Michnick, S. W. Mechanisms and Consequences of Macromolecular Phase Separation. *Cell* **2016**, *165*, 1067–1079.
- (3) Banani, S. F.; Lee, H. O.; Hyman, A. A.; Rosen, M. K. Biomolecular condensates: organizers of cellular biochemistry. *Nat. Rev. Mol. Cell Biol.* **2017**, *18*, 285–298.
- (4) Boeynaems, S.; Alberti, S.; Fawzi, N. L.; Mittag, T.; Polymenidou, M.; Rousseau, F.; Schymkowitz, J.; Shorter, J.; Wolozin, B.; Van Den Bosch, L.; Tompa, P.; Fuxreiter, M. Protein Phase Separation: A New Phase in Cell Biology. *Trends Cell Biol.* **2018**, *28*, 420–435.
- (5) Brangwynne, C. P.; Eckmann, C. R.; Courson, D. S.; Rybarska, A.; Hoege, C.; Gharakhani, J.; Jülicher, F.; Hyman, A. A. Germline P Granules Are Liquid Droplets That Localize by Controlled Dissolution/Condensation. *Science* **2009**, *324*, 1729–1732.
- (6) Hyman, A. A.; Weber, C. A.; Jülicher, F. Liquid-liquid phase separation in biology. *Annu. Rev. Cell Dev. Biol.* **2014**, *30*, 39–58.
- (7) Uversky, V. N. Protein intrinsic disorder-based liquid–liquid phase transitions in biological systems: Complex coacervates and membrane-less organelles. *Adv. Colloid Interface Sci.* **2017**, *239*, 97–114.
- (8) Gomes, E.; Shorter, J. The molecular language of membraneless organelles. *J. Biol. Chem.* **2019**, *294*, 7115–7127.
- (9) Aguzzi, A.; Altmeyer, M. Phase Separation: Linking Cellular Compartmentalization to Disease. *Trends Cell Biol.* **2016**, *26*, 547–558.
- (10) Shin, Y.; Brangwynne, C. P. Liquid phase condensation in cell physiology and disease. *Science* **2017**, *357*, eaaf4382.
- (11) Nott, T. J.; Petsalaki, E.; Farber, P.; Jervis, D.; Fussner, E.; Plochowitz, A.; Craggs, T. D.; Bazett-Jones, D. P.; Pawson, T.; Forman-Kay, J. D.; Baldwin, A. J. Phase Transition of a Disordered Nuage Protein Generates Environmentally Responsive Membraneless Organelles. *Mol. Cell* **2015**, *57*, 936–947.
- (12) Elbaum-Garfinkle, S.; Kim, Y.; Szczepaniak, K.; Chen, C. C.-H.; Eckmann, C. R.; Myong, S.; Brangwynne, C. P. The disordered P granule protein LAF-1 drives phase separation into droplets with

- tunable viscosity and dynamics. *Proc. Natl. Acad. Sci. U. S. A.* **2015**, *112*, 7189–7194.
- (13) Monahan, Z.; Ryan, V. H.; Janke, A. M.; Burke, K. A.; Rhoads, S. N.; Zerze, G. H.; O’Meally, R.; Dignon, G. L.; Conicella, A. E.; Zheng, W.; Best, R. B.; Cole, R. N.; Mittal, J.; Shewmaker, F.; Fawzi, N. L. Phosphorylation of the FUS low-complexity domain disrupts phase separation, aggregation, and toxicity. *EMBO J.* **2017**, *36*, 2951–2967.
- (14) Tompa, P. Intrinsically disordered proteins: a 10-year recap. *Trends Biochem. Sci.* **2012**, *37*, 509–516.
- (15) Romero, P.; Obradovic, Z.; Li, X.; Garner, E. C.; Brown, C. J.; Dunker, A. K. Sequence complexity of disordered protein. *Proteins: Struct., Funct., Bioinf.* **2001**, *42*, 38–48.
- (16) van der Lee, R.; et al. Classification of Intrinsically Disordered Regions and Proteins. *Chem. Rev.* **2014**, *114*, 6589–6631.
- (17) Yang, J.; Zeng, Y.; Liu, Y.; Gao, M.; Liu, S.; Su, Z.; Huang, Y. Electrostatic interactions in the molecular recognition of intrinsically disordered proteins. *J. Biomol. Struct. Dyn.* **2020**, *38*, 4883–4894.
- (18) Koga, S.; Williams, D. S.; Perriman, A. W.; Mann, S. Peptide–nucleotide microdroplets as a step towards a membrane-free protocell model. *Nat. Chem.* **2011**, *3*, 720–724.
- (19) Aumiller, W. M.; Cakmak, F. P.; Davis, B. W.; Keating, C. D. RNA-Based Coacervates as a Model for Membraneless Organelles: Formation, Properties, and Interfacial Liposome Assembly. *Langmuir* **2016**, *32*, 10042–10053.
- (20) Poudyal, R. R.; Cakmak, F. P.; Keating, C. D.; Bevilacqua, P. C. Physical Principles and Extant Biology Reveal Roles for RNA-Containing Membraneless Compartments in Origins of Life Chemistry. *Biochemistry* **2018**, *57*, 2509–2519.
- (21) Spruijt, E.; Westphal, A. H.; Borst, J. W.; Cohen Stuart, M. A.; van der Gucht, J. Binodal Compositions of Polyelectrolyte Complexes. *Macromolecules* **2010**, *43*, 6476–6484.
- (22) Wang, Q.; Schlenoff, J. B. The Polyelectrolyte Complex/Coacervate Continuum. *Macromolecules* **2014**, *47*, 3108–3116.
- (23) McCarty, J.; Delaney, K. T.; Danielsen, S. P. O.; Fredrickson, G. H.; Shea, J.-E. Complete Phase Diagram for Liquid–Liquid Phase Separation of Intrinsically Disordered Proteins. *J. Phys. Chem. Lett.* **2019**, *10*, 1644–1652.
- (24) Dinic, J.; Marciel, A. B.; Tirrell, M. V. Polyampholyte physics: Liquid–liquid phase separation and biological condensates. *Curr. Opin. Colloid Interface Sci.* **2021**, *54*, 101457.
- (25) Perry, S.; Li, Y.; Priftis, D.; Leon, L.; Tirrell, M. The Effect of Salt on the Complex Coacervation of Vinyl Polyelectrolytes. *Polymers* **2014**, *6*, 1756–1772.
- (26) Li, L.; Srivastava, S.; Andreev, M.; Marciel, A. B.; de Pablo, J. J.; Tirrell, M. V. Phase Behavior and Salt Partitioning in Polyelectrolyte Complex Coacervates. *Macromolecules* **2018**, *51*, 2988–2995.
- (27) Adhikari, S.; Leaf, M. A.; Muthukumar, M. Polyelectrolyte complex coacervation by electrostatic dipolar interactions. *J. Chem. Phys.* **2018**, *149*, 163308.
- (28) Ali, S.; Bleuel, M.; Prabhu, V. M. Lower Critical Solution Temperature in Polyelectrolyte Complex Coacervates. *ACS Macro Lett.* **2019**, *8*, 289–293.
- (29) Adhikari, S.; Prabhu, V. M.; Muthukumar, M. Lower Critical Solution Temperature Behavior in Polyelectrolyte Complex Coacervates. *Macromolecules* **2019**, *52*, 6998–7004.
- (30) Ye, Z.; Sun, S.; Wu, P. Distinct Cation–Anion Interactions in the UCST and LCST Behavior of Polyelectrolyte Complex Aqueous Solutions. *ACS Macro Lett.* **2020**, *9*, 974–979.
- (31) Kumar, R.; Audus, D.; Fredrickson, G. H. Phase Separation in Symmetric Mixtures of Oppositely Charged Rodlike Polyelectrolytes. *J. Phys. Chem. B* **2010**, *114*, 9956–9976.
- (32) Rumyantsev, A. M.; de Pablo, J. J. Liquid Crystalline and Isotropic Coacervates of Semiflexible Polyanions and Flexible Polycations. *Macromolecules* **2019**, *52*, 5140–5156.
- (33) Shakya, A.; Girard, M.; King, J. T.; Olvera de la Cruz, M. Role of chain flexibility in asymmetric polyelectrolyte complexation in salt solutions. *Macromolecules* **2020**, *53*, 1258–1269.
- (34) Lytle, T. K.; Sing, C. E. Tuning chain interaction entropy in complex coacervation using polymer stiffness, architecture, and salt valency. *Mol. Syst. Des. Eng.* **2018**, *3*, 183–196.
- (35) Horn, J.; Kapelner, R.; Obermeyer, A. Macro- and Microphase Separated Protein-Polyelectrolyte Complexes: Design Parameters and Current Progress. *Polymers* **2019**, *11*, 578.
- (36) Perry, S. L.; Sing, C. E. 100th Anniversary of Macromolecular Science Viewpoint: Opportunities in the Physics of Sequence-Defined Polymers. *ACS Macro Lett.* **2020**, *9*, 216–225.
- (37) Pak, C. W.; Kosno, M.; Holehouse, A. S.; Padrick, S. B.; Mittal, A.; Ali, R.; Yunus, A. A.; Liu, D. R.; Pappu, R. V.; Rosen, M. K. Sequence Determinants of Intracellular Phase Separation by Complex Coacervation of a Disordered Protein. *Mol. Cell* **2016**, *63*, 72–85.
- (38) Schuster, B. S.; Dignon, G. L.; Tang, W. S.; Kelley, F. M.; Ranganath, A. K.; Jahnke, C. N.; Simpkins, A. G.; Regy, R. M.; Hammer, D. A.; Good, M. C.; Mittal, J. Identifying sequence perturbations to an intrinsically disordered protein that determine its phase-separation behavior. *Proc. Natl. Acad. Sci. U. S. A.* **2020**, *117*, 11421–11431.
- (39) Chang, L.-W.; Lytle, T. K.; Radhakrishna, M.; Madinya, J. J.; Vélez, J.; Sing, C. E.; Perry, S. L. Sequence and entropy-based control of complex coacervates. *Nat. Commun.* **2017**, *8*, 1273.
- (40) Protter, D. S.; Parker, R. Principles and Properties of Stress Granules. *Trends Cell Biol.* **2016**, *26*, 668–679.
- (41) Feric, M.; Vaidya, N.; Harmon, T. S.; Mitrea, D. M.; Zhu, L.; Richardson, T. M.; Kriwacki, R. W.; Pappu, R. V.; Brangwynne, C. P. Coexisting Liquid Phases Underlie Nucleolar Subcompartments. *Cell* **2016**, *165*, 1686–1697.
- (42) Sanders, D. W.; et al. Competing Protein-RNA Interaction Networks Control Multiphase Intracellular Organization. *Cell* **2020**, *181*, 306–324.e28.
- (43) Lafontaine, D. L. J.; Riback, J. A.; Bascetin, R.; Brangwynne, C. P. The nucleolus as a multiphase liquid condensate. *Nat. Rev. Mol. Cell Biol.* **2021**, *22*, 165–182.
- (44) Mountain, G. A.; Keating, C. D. Formation of multiphase complex coacervates and partitioning of biomolecules within them. *Biomacromolecules* **2020**, *21*, 630–640.
- (45) Lu, T.; Spruijt, E. Multiphase complex coacervate droplets. *J. Am. Chem. Soc.* **2020**, *142*, 2905–2914.
- (46) Jing, H.; Bai, Q.; Lin, Y.; Chang, H.; Yin, D.; Liang, D. Fission and internal fusion of protocell with membraneless “organelles” formed by liquid–liquid phase separation. *Langmuir* **2020**, *36*, 8017–8026.
- (47) Chen, Y.; Yuan, M.; Zhang, Y.; Liu, S.; Yang, X.; Wang, K.; Liu, J. Construction of coacervate-in-coacervate multi-compartment protocells for spatial organization of enzymatic reactions. *Chem. Sci.* **2020**, *11*, 8617–8625.
- (48) Overbeek, J. T. G.; Voorn, M. J. Phase separation in polyelectrolyte solutions. theory of complex coacervation. *J. Cell. Comp. Physiol.* **1957**, *49*, 7–26.
- (49) Sing, C. E. Development of the modern theory of polymeric complex coacervation. *Adv. Colloid Interface Sci.* **2017**, *239*, 2–16.
- (50) Castelnovo, M.; Joanny, J.-F. Complexation between oppositely charged polyelectrolytes: Beyond the Random Phase Approximation. *Eur. Phys. J. E* **2001**, *6*, 377–386.
- (51) Kudlay, A.; Olvera de la Cruz, M. Precipitation of oppositely charged polyelectrolytes in salt solutions. *J. Chem. Phys.* **2004**, *120*, 404–412.
- (52) Kudlay, A.; Ermoshkin, A. V.; Olvera de la Cruz, M. Complexation of Oppositely Charged Polyelectrolytes: Effect of Ion Pair Formation. *Macromolecules* **2004**, *37*, 9231–9241.
- (53) Qin, J.; de Pablo, J. J. Criticality and Connectivity in Macromolecular Charge Complexation. *Macromolecules* **2016**, *49*, 8789–8800.
- (54) Lee, J.; Popov, Y. O.; Fredrickson, G. H. Complex coacervation: A field theoretic simulation study of polyelectrolyte complexation. *J. Chem. Phys.* **2008**, *128*, 224908.
- (55) Lytle, T. K.; Sing, C. E. Transfer matrix theory of polymer complex coacervation. *Soft Matter* **2017**, *13*, 7001–7012.

- (56) Zhang, P.; Alsaifi, N. M.; Wu, J.; Wang, Z.-G. Salting-out and salting-in of polyelectrolyte solutions: a liquid-state theory study. *Macromolecules* **2016**, *49*, 9720–9730.
- (57) Zhang, P.; Alsaifi, N. M.; Wu, J.; Wang, Z.-G. Polyelectrolyte complex coacervation: effects of concentration asymmetry. *J. Chem. Phys.* **2018**, *149*, 163303.
- (58) Shen, K.; Wang, Z.-G. Electrostatic correlations and the polyelectrolyte self energy. *J. Chem. Phys.* **2017**, *146*, 084901.
- (59) Shen, K.; Wang, Z.-G. Polyelectrolyte chain structure and solution phase behavior. *Macromolecules* **2018**, *51*, 1706–1717.
- (60) Perry, S. L.; Sing, C. E. PRISM-based theory of complex coacervation: excluded volume versus chain correlation. *Macromolecules* **2015**, *48*, 5040–5053.
- (61) Rubinstein, M.; Liao, Q.; Panyukov, S. Structure of liquid coacervates formed by oppositely charged polyelectrolytes. *Macromolecules* **2018**, *51*, 9572–9588.
- (62) Borue, V. Y.; Erukhimovich, I. Y. A statistical theory of weakly charged polyelectrolytes: fluctuations, equation of state and micro-phase separation. *Macromolecules* **1988**, *21*, 3240–3249.
- (63) Castelnovo, M.; Joanny, J.-F. Formation of Polyelectrolyte Multilayers. *Langmuir* **2000**, *16*, 7524–7532.
- (64) Wittmer, J.; Johner, A.; Joanny, J. F. Random and Alternating Polyampholytes. *EPL* **1993**, *24*, 263–268.
- (65) Rumyantsev, A. M.; Jackson, N. E.; Yu, B.; Ting, J. M.; Chen, W.; Tirrell, M. V.; de Pablo, J. J. Controlling Complex Coacervation via Random Polyelectrolyte Sequences. *ACS Macro Lett.* **2019**, *8*, 1296–1302.
- (66) Lin, Y.-H.; Forman-Kay, J. D.; Chan, H. S. Sequence-Specific Polyampholyte Phase Separation in Membraneless Organelles. *Phys. Rev. Lett.* **2016**, *117*, 178101.
- (67) Lin, Y.-H.; Song, J.; Forman-Kay, J. D.; Chan, H. S. Random-phase-approximation theory for sequence-dependent, biologically functional liquid-liquid phase separation of intrinsically disordered proteins. *J. Mol. Liq.* **2017**, *228*, 176–193.
- (68) Lin, Y.-H.; Brady, J. P.; Forman-Kay, J. D.; Chan, H. S. Charge pattern matching as a 'fuzzy' mode of molecular recognition for the functional phase separations of intrinsically disordered proteins. *New J. Phys.* **2017**, *19*, 115003.
- (69) Wessén, J.; Pal, T.; Das, S.; Lin, Y.-H.; Chan, H. S. A Simple Explicit-Solvent Model of Polyampholyte Phase Behaviors and Its Ramifications for Dielectric Effects in Biomolecular Condensates. *J. Phys. Chem. B* **2021**, *125*, 4337–4358.
- (70) Rumyantsev, A. M.; Jackson, N. E.; Johner, A.; de Pablo, J. J. Scaling Theory of Neutral Sequence-Specific Polyampholytes. *Macromolecules* **2021**, *54*, 3232–3246.
- (71) Amin, A. N.; Lin, Y.-H.; Das, S.; Chan, H. S. Analytical Theory for Sequence-Specific Binary Fuzzy Complexes of Charged Intrinsically Disordered Proteins. *J. Phys. Chem. B* **2020**, *124*, 6709–6720.
- (72) Danielsen, S. P. O.; McCarty, J.; Shea, J.-E.; Delaney, K. T.; Fredrickson, G. H. Molecular design of self-coacervation phenomena in block polyampholytes. *Proc. Natl. Acad. Sci. U. S. A.* **2019**, *116*, 8224–8232.
- (73) Danielsen, S. P. O.; McCarty, J.; Shea, J.-E.; Delaney, K. T.; Fredrickson, G. H. Small ion effects on self-coacervation phenomena in block polyampholytes. *J. Chem. Phys.* **2019**, *151*, 034904.
- (74) Fu, J.; Schlenoff, J. B. Driving forces for oppositely charged polyion association in aqueous solutions: enthalpic, entropic, but not electrostatic. *J. Am. Chem. Soc.* **2016**, *138*, 980–990.
- (75) Rathee, V. S.; Sidky, H.; Sikora, B. J.; Whitmer, J. K. Role of associative charging in the entropy–energy balance of polyelectrolyte complexes. *J. Am. Chem. Soc.* **2018**, *140*, 15319–15328.
- (76) Lytle, T. K.; Chang, L.-W.; Markiewicz, N.; Perry, S. L.; Sing, C. E. Designing Electrostatic Interactions via Polyelectrolyte Monomer Sequence. *ACS Cent. Sci.* **2019**, *5*, 709–718.
- (77) Madinya, J. J.; Chang, L.-W.; Perry, S. L.; Sing, C. E. Sequence-dependent self-coacervation in high charge-density polyampholytes. *Mol. Syst. Des. Eng.* **2020**, *5*, 632–644.
- (78) Sing, C. E. Micro- to macro-phase separation transition in sequence-defined coacervates. *J. Chem. Phys.* **2020**, *152*, 024902.
- (79) Simon, J. R.; Carroll, N. J.; Rubinstein, M.; Chilkoti, A.; López, G. P. Programming molecular self-assembly of intrinsically disordered proteins containing sequences of low complexity. *Nat. Chem.* **2017**, *9*, 509–515.
- (80) Sear, R. P.; Cuesta, J. A. Instabilities in complex mixtures with a large number of components. *Phys. Rev. Lett.* **2003**, *91*, 245701.
- (81) Jacobs, W. M.; Frenkel, D. Predicting phase behavior in multicomponent mixtures. *J. Chem. Phys.* **2013**, *139*, 024108.
- (82) Mao, S.; Kuldinow, D.; Haataja, M. P.; Košmrlj, A. Phase behavior and morphology of multicomponent liquid mixtures. *Soft Matter* **2019**, *15*, 1297–1311.
- (83) Mao, S.; Chakraverti-Wuerthwein, M. S.; Gaudio, H.; Košmrlj, A. Designing the morphology of separated phases in multicomponent liquid mixtures. *Phys. Rev. Lett.* **2020**, *125*, 218003.
- (84) Chen, X.; Chen, E.-Q.; Shi, A.-C.; Yang, S. Multiphase Coacervates Driven by Electrostatic Correlations. *ACS Macro Lett.* **2021**, *10*, 1041–1047.
- (85) Borue, V. Y.; Erukhimovich, I. Y. A statistical theory of globular polyelectrolyte complexes. *Macromolecules* **1990**, *23*, 3625–3632.
- (86) Mahdi, K. A.; Olvera de la Cruz, M. Phase Diagrams of Salt-Free Polyelectrolyte Semidilute Solutions. *Macromolecules* **2000**, *33*, 7649–7654.
- (87) Barber, C. B.; Dobkin, D. P.; Huhdanpaa, H. The quickhull algorithm for convex hulls. *ACM Trans. Math. Software* **1996**, *22*, 469–483.
- (88) Wolff, J.; Marques, C. M.; Thalmann, F. Thermodynamic Approach to Phase Coexistence in Ternary Phospholipid-Cholesterol Mixtures. *Phys. Rev. Lett.* **2011**, *106*, 128104.
- (89) Yu, B.; Rumyantsev, A. M.; Jackson, N. E.; Liang, H.; Ting, J. M.; Meng, S.; Tirrell, M. V.; de Pablo, J. J. Complex coacervation of statistical polyelectrolytes: role of monomer sequences and formation of inhomogeneous coacervates. *Mol. Syst. Des. Eng.* **2021**, *6*, 790–804.
- (90) Boeynaems, S.; Holehouse, A. S.; Weinhardt, V.; Kovacs, D.; Van Lindt, J.; Larabell, C.; Van Den Bosch, L.; Das, R.; Tompa, P. S.; Pappu, R. V.; Gitler, A. D. Spontaneous driving forces give rise to protein-RNA condensates with coexisting phases and complex material properties. *Proc. Natl. Acad. Sci. U. S. A.* **2019**, *116*, 7889–7898.
- (91) Donau, C.; Späth, F.; Stasi, M.; Bergmann, A. M.; Boekhoven, J. Phase Transitions in Chemically Fueled, Multiphase Complex Coacervate Droplets. *Angew. Chem., Int. Ed.* **2022**, *61*, e202211905.